Thermo-mechanical modeling of a filled elastomer based on the physics of mobility reduction

Davide Colombo, Hélène Montes, François Lequeux, Sabine Cantournet

Thermo-mechanical modeling of a filled elastomer based on the physics of mobility reduction

Davide Colombo[a], Hélène Montes[b], François Lequeux[b], Sabine Cantournet[a]*

[a]MINES ParisTech, PSL-Research University, MAT - Centre des Matériaux, CNRS UMR 7633, BP 87 91003 Evry, France

[b]CNRS UPMC ESPCI ParisTech PSL Res Univ, Lab. SIMM, UMR 7615, F-75231 Paris, France}

*corresponding author: sabine.cantournet@mines-paristech.fr

Abstract

The addition of rigid fillers to an elastomeric matrix enhances its mechanical properties. This reinforcement effect is primarily due to a filler network structure in which polymer regions between aggregates play the principal role. In this study, a continuum constitutive equation is formulated for polymer behavior under strong confinement conditions. This behavior can be accounted for by a local glass transition temperature that combines the effects of physical interaction and stress softening in a unique viscoelastic formulation. The model reproduces, at a microscopic scale, the processes governing the Payne effect, including the temperature dependence of the viscoelastic behavior of the filled elastomer reinforcement.

Keywords: filled elastomer, Payne effect, glassy bridge, reinforcement, confinement, chain mobility

1 Introduction

The reinforcement of rubbers with silica or carbon black nano-fillers (particles with diameters of 5–30 nm aggregated into particles with diameters of 100 nm–1 μm) is unique for many reasons. Research concerning the enhancement of properties has particularly focused on the stiffness, the strain and stress at rupture, and the wear resistance (Mark et al., 2013). The nanoscopic aggregates introduce new dependencies and non-linearities to the mechanical response of the matrix.

The effects of frequency and temperature are very different for pure rubber and reinforced rubber (Drozdov and Dorfmann, 2002; Berriot et al., 2002; Fritzsche and Klüppel, 2011). The former is efficiently described by the entropic elasticity of Gaussian chains (Treloar,

2005), while filled rubber has a rather enthalpic-like evolution with temperature (Clement et al., 2005). Moreover, the addition of fillers results in early non-linear responses as compared with the unreinforced matrix. For instance, under cyclic loading of increasing amplitude, filled elastomers show a drop in storage modulus and a peak in loss modulus. This strain amplitude dependence is referred to as the Payne effect (Payne, 1962). As the concentration increases, the phenomenon becomes more evident. However, the effect can be observed at very low concentrations, below the percolation threshold, as observed by Cassagnau et al. for filler fractions less than 5% by volume (Cassagnau, 2003). Moreover, the influence of the reinforcement depends slightly on the mechanical properties of the nano-aggregates but is extremely sensitive to the morphology of the system (Montes et al, 2010), i.e., the spatial arrangement of the phases and the nature of the interactions between matrix and filler (Ramier et al, 2007).

When this peculiar behavior was first studied, Payne (Payne, 1962) supported the idea that it was due to a distribution of hard and soft zones within the material. According to Payne, "*the rubber at very low strains could be regarded as possessing a maximum content of hard zones.*" The temperature would influence the equilibrium between soft and hard zones and "*with increasing strain, a yield point may be said to exist.*" Finally, "*the proportion of hard and soft zones is determined by the type and concentration, the details of processing and the immediate preceding strain history.*"

Today, it is known that the reinforcement is the expression of a structural phenomenon. A fractal network is developed in the system (Huber et al., 1996) and can be disrupted by an applied stress. Kraus (Kraus, 1984) used the concept of destruction and reorganization of a carbon-black network to build a model that describes the Payne effect. Further developments (Huber et al., 1996) led to the definition of a fractal network of fillers, the connectivity of which determines the stiffness evolution of the composite. Maier and Göritz (Maier and Göritz, 1996) proposed a different interpretation based on the adsorption–desorption of polymer chains on the filler surface. Other authors (Funt, 1988) considered the entanglement density in the surrounding aggregate to play a major role on the temperature and Payne dependence. The connections governing the clustering are polymer regions confined between the surfaces of particles, which, as a consequence of their confinement, have specific mechanical properties different from those of the bulk polymer (Klüppel, 2003). The thicknesses of these polymer bridges are a few nanometers

(Medalia, 1986). Because the confinement is strong in these regions, the filler surfaces affect the polymer properties, resulting in behaviors of filled elastomers that are different from that of the bulk rubber.

For all of these theories, the key concepts are either the presence of a filler network within the matrix or an interphase or fundamental interfacial phenomena on the chain properties in the filler surface neighborhood. The effect of surface on the macromolecule dynamics and mechanics has been amply discussed in the literature (Vogt, 2018). In the presence of a free surface, thin polymer layers show a shift in glass transition temperature, which can reach values up to 60 K for film layers thinner than 40 nm (Wallace et al., 1995). This phenomenon occurs because the free surface increases the degrees of freedom of polymer chains, thus increasing their mobility. Similar behavior is observed when the polymer is in contact with a surface with a weak or repulsive interaction (Forrest et al., 1997), while in the case of a strongly attractive interaction, the behavior is just the opposite (Van Zanten et al., 1996). The latter condition corresponds to the situation of filled elastomers. Thus, within confined regions, the filler-matrix interaction introduces constraints on the chain dynamics and reduces polymer mobility (Nguyen et al., 2019, 2018; Cheng et al., 2017; Batistakis et al., 2014; Mujtaba, 2014, Klüppel, 2008, Papakonstantopoulos et al., 2007; Heinrich and Klüppel, 2004).

In this study, it will be assumed that the slowing down of the polymer chain dynamics can be described by a glass transition temperature that depends on the distance from the surface of the closest particles. As a consequence, the solid particles are considered to be connected mechanically with glassy bridges (Montes et al., 2003), which creates a network, the connectivity of which depends on temperature, internal morphology, and external forces.

Many approaches can be found in the literature to describe the physical processes involved within a constitutive continuum mechanics equation. One method is to include elements of this reinforcement scenario to build a phenomenological law (Martinez et al., 2011; Lion and Kardelky, 2004; Cantournet et al., 2009). Another technique is to start from a thermodynamic representation of the clustering and deduce a constitutive law depending on the hard zone/soft zone equilibrium (Klüppel, 2003). A different micro-mechanical approach computes the effective properties of a multi-phase system knowing the concentrations and the physical-geometrical features of the phases. This prediction is

obtained either by analytical approximation (Marcadon et al., 2007) or by numerical testing of representative volumes (Jean et al., 2011; Sodhani and Reese, 2014). These techniques are limited primarily because they require the mechanical properties of the polymer chains at the interface as an input. Because the small-scale length hinders their experimental characterization, it is difficult to find data in the literature (Wood et al., 2015). In many cases, homogenization models use the interphase stiffness as a tunable parameter (Deng et al., 2012; Omnès et al, 2008).

In this paper, we propose a continuum model to describe the mechanical behavior of the polymer at this inter-phase. Two main features characterize this model. First, the model accounts for the influence of the filler-matrix interaction: it describes explicitly the modification of the polymer dynamics as a variation of the glass transition temperature induced by the closest solid surfaces. In addition to a structural short range modification that will be neglected here (Berriot et al., 2002; Merabia et al., 2008), the confinement induces a gradient of properties in the system. In this work, we choose to describe this effect using a gradient of the glass transition temperature near the filler surface. This picture has already been confirmed to be efficient for describing the dynamics of polymer chains in filled elastomers (Papon et al., 2012). Second, non-linear mechanical properties will be included. A "pseudo"-plasticity of the glassy polymer has been reported in the literature (Robertson, 1966). In the present study, the "pseudo"-plasticity will be described as a shift in mobility under pressure and deviatoric stress. This approach results in the coupling of physical interactions and thermal and mechanical activation in a single parameter that defines the variation from the glass transition of the unfilled polymer and quantifies the polymer mobility. This dependency is included in a three-dimensional non-linear viscoelastic law and is implemented in a finite element code. Finally, the physical parameters included in the model are those of the fillers and of the pure matrix.

The paper is organized as follows. First, the local viscoelastic equation is introduced as a time–temperature dependent relation. Second, the reduction in mobility of polymer chains induced by filler-matrix interactions is described in terms of the glass transition temperature gradient. Next, a simple law for the non-linear mechanics of a glassy polymer is established. Indeed, all contributions to the mechanical response are controlled by a stress-dependent relaxation time. Then, the two dependencies are coupled together to integrate the effects of temperature and stress in a single formulation. The cyclic response

of a confined region in the polymer can be addressed. Finally, this model is extended to describe the behavior of real filled rubber, with a discussion of the role of disorder, which may be an important ingredient. The results show that the model can reproduce, at a microscopic scale, the main characteristics of filler reinforcement experienced at the macroscopic scale.

2 Local viscoelastic behavior of polymer

The mechanical response of bulk polymer chains is driven by entropic callback forces at temperatures much higher than the bulk glass transition temperature T_g^{bulk} (Treloar, 2005). In the rubber state, dissipation is negligible, and the macroscopic behavior is reproduced by hyperelastic laws, with stiffness coefficients on the order of MPa (Boyce and Arruda, 2000; Cantournet et al., 2007). Furthermore, polymer chains are in the glassy state at temperatures lower than T_g^{bulk}, exhibiting low dissipation and stiffness on the order of GPa. The transition between the two regimes is viscoelastic. Experimentally, a wide spectrum of relaxation times is observed in the glassy-to-rubbery transition, and more sophisticated models are able to account for these intrinsic dynamic heterogeneities in bulk polymers (Masurel et al., 2015).

In filled rubbers, the degree of confinement of polymer chains between filler surfaces is distributed. As a result, the distribution of relaxation times in a filled rubber is wider than it is in the bulk polymer matrix. For the sake of simplicity, we will thus assume that the viscoelastic response of polymer chains can be described, in a first approximation, by a single relaxation time. In this work, we have limited ourselves to the alpha transition. We do not consider the secondary movements associated with the beta relaxation.

Adding fillers modifies the local polymer properties. The stress–strain relationship in a filled elastomer is highly non-linear, even in the small-strain range. At small strains, filled systems show a decreasing complex modulus with increasing temperature (Wang, 1998; Berriot et al., 2002; Fritzsche and Klüppel, 2011), opposite to the increasing one of the pure matrix predicted by entropic elasticity (Treloar, 2005). Another peculiar feature of filled elastomers is their non-linear behavior with dynamic strain, called the Payne effect (Payne, 1962). For increasing strain amplitudes, the first-order storage modulus exhibits a decrease, even for strains smaller than 10%. At the same strain values, the loss modulus

reaches a maximum. For the sake of simplicity, the new constitutive model is then developed within the small-strain framework.

An attractive filler-matrix interaction reduces the degrees of freedom of the chains surrounding the filler surfaces. Configurational constraints induce an increase in the energy barrier for chain motions, which can be accounted for by an increase in the glass transition temperature of polymer chains at the interface with respect to the bulk matrix (Wallace et al., 1995). Chains in the vicinity of the filler surface behave as glassy polymers, with low dissipation and stiffness close to 1 GPa. Farther away from the surface, the influence of this interaction on the matrix properties decreases, and a continuum gradient of viscoelastic behaviors has been proposed to describe the mechanical response of polymer chains within the material (Berriot et al., 2003).

Thus, the matrix viscoelastic behavior can be described with a two-branch (Zener) model (see Fig. 1). In the time-independent branch, a rubbery elastic low-modulus term represents the pure matrix bulk behavior. In the time-dependent branch, a glassy elastic large-modulus term is coupled with a local relaxation time, $\tau(z_i, T, \boldsymbol{\sigma})$, which is function of temperature T, the distance from the surface filler z_i, and local stress tensor $\boldsymbol{\sigma}$. The rubbery component, resulting from the entropy variation of polymer chains, is proportional to the absolute temperature. However, its variation is much weaker than that of the glassy branch and will be neglected. For the sake of simplicity, the material is considered to be isotropic and quasi-incompressible (Poisson's ratio $\nu = 0.49$). The same relaxation time is imposed on the deviatoric and volumetric parts of the response.

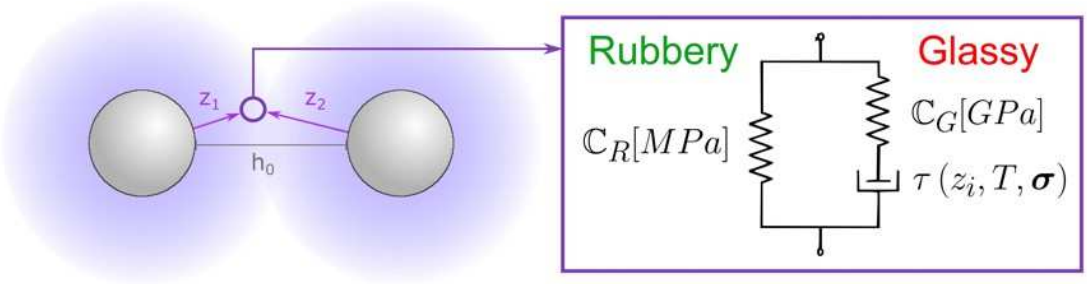

Figure 1: Within the glassy bridge, there is a local non-linear viscoelasticity law scheme.

Therefore, the local behavior is described by the differential equation

$$\tau(z_i, T, \boldsymbol{\sigma})\, \dot{\boldsymbol{\sigma}} + \boldsymbol{\sigma} = \mathbb{C}_R : \boldsymbol{\varepsilon} + \tau(z_i, T, \boldsymbol{\sigma})(\mathbb{C}_R + \mathbb{C}_G) : \dot{\boldsymbol{\varepsilon}}\,, \quad (1)$$

where $\mathbb{C}_R$ and $\mathbb{C}_G$ are the isotropic stiffness tensors for the elastic rubbery and glassy responses, respectively. The elastic Young's moduli are respectively called E_R and E_G. The $(\dot{*})$ stands for the time derivative. Our model considers the frequency dependence of the viscoelastic response of the polymer chains. In Eq. (1), the second contribution of the right part of the equation depends on the strain rate $(\dot{\boldsymbol{\varepsilon}})$, i.e., on the frequency.

In the case where the relaxation time τ is constant in time, the relaxation function reduces to an exponential function and the stress time function can be written as

$$\boldsymbol{\sigma}(t) = \mathbb{C}_R : \boldsymbol{\varepsilon}(t) + \int_{-\infty}^{t} \mathbb{C}_G e^{-\frac{t-t'}{\tau(z_i, T, \boldsymbol{\sigma})\, \dot{\sigma}}} : \dot{\boldsymbol{\varepsilon}}(t') dt' \quad (2)$$

In the case of non-linear viscoelasticity, the relaxation time $\tau(z_i,\ T,\ \boldsymbol{\sigma})$ is a function of the local stress and strain, which depend on time. Exact solutions for the differential equation may be formulated using reduced time (Schapery, 1969).

If the time increments are sufficiently small, it is convenient to work with the linear viscoelastic formulation (Simo and Hughes, 2006) and to reset at each step of the relaxation time τ^{k+1} at time t^{k+1}, as a function of the variable at the previous time t^k. In other words, the relaxation time is computed at the beginning of each increment and held constant over the increment. This numerical approach has been chosen for the remainder of the article.

The relaxation times depend on the temperature, following the classical William–Landel–Ferry (WLF) function (Ferry, 1980) with respect to the local glass transition temperature

$$\log_{10}\left[\frac{\tau(z_i, T, \boldsymbol{\sigma})}{\tau_g}\right] = -\frac{C_1[T - T_g(z_i, \boldsymbol{\sigma})]}{C_2 + [T - T_g(z_i, \boldsymbol{\sigma})]} = \mathcal{G}_{wlf}\left(T - T_g(z_i, \boldsymbol{\sigma})\right), \quad (3)$$

where the relaxation time τ_g at the bulk polymer glass transition is set to 1 s (Ferry, 1980) and C_1 and C_2 are bulk matrix parameters. The function $\mathcal{G}_{wlf}$ is introduced to lighten the following equations. Moreover, we also assume that C_1 and C_2 are constant for any value of $T_g(z, \boldsymbol{\sigma})$, our $T_g(z, \boldsymbol{\sigma})$ being defined at 1 s.

In this work, numerical calculations have been performed using the values C_1 =12.8 and C_2 = 34.0 K, which were chosen from a reference glass transition temperature of T_g^{bulk} = 150 K, which corresponds to a polydimethylsiloxane (PDMS) matrix.

In our model, the mechanical response of the bridge is controlled by the local relaxation time $(z_i, T, \boldsymbol{\sigma})$, which only depends on the difference $\left(T - T_g(z_i, \boldsymbol{\sigma})\right)$ defined at 1 s (see Eq. (3)). If we consider a bulk matrix ($z_i = \infty$), its relaxation time, $\tau(z_i, T, \boldsymbol{\sigma})$ at rest ($\boldsymbol{\sigma} = \boldsymbol{0}$) is determined by $\left(T - T_g^{bulk}\right)$, the difference between the temperature T and the glass transition temperature T_g^{bulk} at 1 s. The local relaxation time does not depend on the frequency. The frequency dependence of the mechanical response of a bulk matrix is taken into account by the strain rate term $\dot{\boldsymbol{\varepsilon}}$ included in Eq. (1).

The model accounts for the evolution of the properties using a local glass transition temperature $T_g(z_i, \boldsymbol{\sigma})$ that depends on the distance from particle surface and the local stress tensor. An isothermal system has been assumed, and self-heating is neglected. The model does not consider the effects of physical ageing.

As the distance decreases, the glass transition temperature increases; as a result, the stiffness increases in the vicinity of the surface. Stress dependence is a specific way to reproduce "pseudo"-plastic behavior in bulk glassy polymers (Buckley and Jones, 1995). Mechanical energy induces variations in the polymer chain conformation, leading to flow-like phenomenon. Because the latter is dependent on a characteristic time, stress results in a decrease in the evolution time, as predicted by the Eyring model (Ree and Eyring, 1955).

The following sections present in detail the mathematical expressions describing both dependences.

2.1 Surface distance dependence of the glass transition temperature – $T_g(z_i)$

From the literature (Long and Lequeux, 2001; Berriot et al, 2002; Keddie et al, 1994), a continuous function of $T_g(z)$ has been used to reproduce the local increase in the glass transition temperature within the vicinity of the particle surface

$$T_g(z) = T_g^{bulk}\left(1 + \frac{\delta}{z}\right), \quad (4)$$

where δ is a characteristic length of the filler-matrix interaction in the order of a nanometer, z is the distance from the particle surface, and T_g^{bulk} is the bulk glass transition temperature.

In the case of a polymer confined between two rigid surfaces, i.e., two aggregate surfaces, it will be assumed that the local glass transition can be approximated by the sum of two contributions (see Fig. 1).

$$T_g(z_i) = T_g(z_1, z_2) = T_g^{bulk}\left(1 + \frac{\delta}{z_1} + \frac{\delta}{z_2}\right) \quad (5)$$

Thus, Eq. (5), combined with Eq. (3), defines a relaxation time space distribution for the matrix confined between two neighboring particles. Consequently, the distribution of the relaxation times of polymer chains is spread over several decades. In between the two spherical particles, the middle point of the bridge is the saddle point of the relaxation time spatial distribution. The middle point of the bridge is then the softer segment of the symmetry axis and simultaneously the most rigid point in the symmetry plane of the bridge (see Fig. 2). For these reasons, the new model has been analyzed particularly at the middle point, $z_1 = z_2 = h_0/2$, where h_0 is the gap between the two neighboring particles of interest (see section 3).

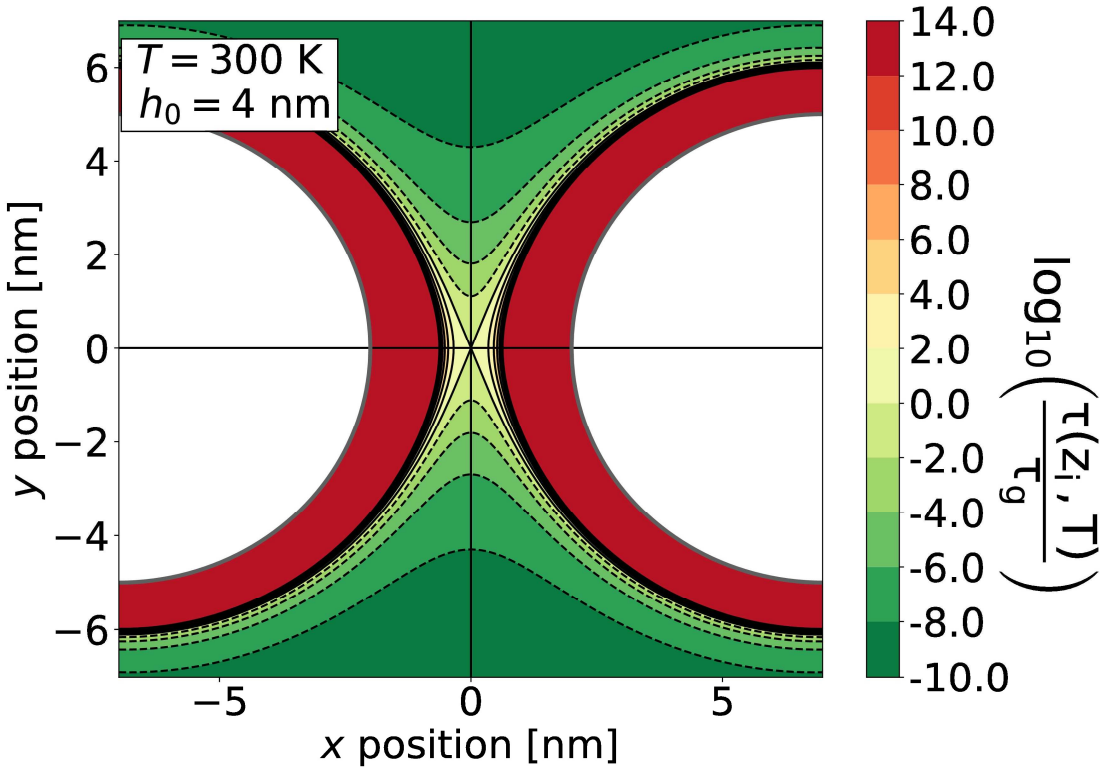

Figure 2: Relaxation time gradient ($\log_{10}$): radial section of a glassy bridge at $T = T_g^{bulk} + 150$ K, centered on the middle point of the axis connecting two particles (white) of radius r of 5 nm and at a distance h_0 of 4 nm. Relaxation times were computed applying Eq. (3) and Eq. (5) with $T_g^{bulk} = 150$ K, $C_1 = 12.8$, $C_2 = 34.0$ K, and $\delta = 1$ nm. $z_1 = \sqrt{(x + h_0 + r)^2 + y^2} - r$ and $z_2 = \sqrt{(x + h_0 + r)^2 + y^2} + r$.

2.2 Stress dependence of the glass transition temperature—$T_g(\sigma)$

Under mechanical work, as in uni-axial or shear tests, the bulk polymer shows a yielding behavior at $T < T_g^{bulk}$. As the stress approaches the yield stress, the polymer chains deviate from the elastic response to undergo a flow process that originates from an enhancement of the mobility of the amorphous macromolecules (Loo et al., 2000; Lee and Ediger, 2010). Thus, we assume that the flow-like behavior results in a shift in the glass transition temperature.

The idea of a glass transition temperature that depends on the loading state is not original. Experimental evidence for bulk polymer glasses can be found in the literature (Andrews and Kazama, 1967; Zhou et al., 1995). Moreover, the glass transition temperature is commonly known to vary with the pressure p (Ferry, 1980). A constant material parameter α_p is thus defined by

$$\frac{\partial T_g}{\partial p} = \alpha_p \qquad (6)$$

α_p can be obtained by PVT measurement[1] and has typical values near 0.2 MPa^{-1} (Ferry, 1980).

To consider the volumetric and deviatoric parts of the stress, we rather propose to apply a Drucker–Prager criterion, as in performed by Rottler and Robbins (Rottler and Robbins, 2001). The Drucker–Prager criterion is imposed directly as a shift in the glass transition.

$$T_g(\boldsymbol{\sigma}) = T_g^{bulk}(\boldsymbol{\sigma} = \mathbf{0}) - f(\boldsymbol{\sigma}) = T_g^{bulk}(\boldsymbol{\sigma} = \mathbf{0}) - \frac{\sqrt{\frac{3}{2}\boldsymbol{\sigma}_{dev} : \boldsymbol{\sigma}_{dev}} - \alpha\, p}{K}, \qquad (7)$$

where $\boldsymbol{\sigma}_{dev}$ is the deviatoric part of the stress $\boldsymbol{\sigma}$ and p is the pressure, related by $\boldsymbol{\sigma} = \boldsymbol{\sigma}_{dev} - p\mathbf{I}$ and $p = -\frac{1}{3}Tr(\boldsymbol{\sigma})$. The K parameter is directly related to the stress at yield, as developed in the following. The parameter $\alpha = \alpha_p/K$ varies typically between 0.01 and 0.3, and K is on the order of 1 MPa^{-1} K^{-1}. The model has been implemented in 1D (Python internal code) and 3D (finite element, Z-set, www.zset-software.com) formulations with identical results. We used $T_g^{bulk} = 150\ K$, K= 1 MPa K^{-1}, and α= 0.3 for the following.

If the polymer sample undergoes a constant strain rate $\dot{\boldsymbol{\varepsilon}}$, the model predicts a temperature and rate dependence of the stress that can be approximated to the classical Eyring relation below the glass transition temperature. In that case, the yield stress depends weakly on time ($\dot{\boldsymbol{\sigma}} \approx 0$) and its value, called σ_Y, is nearly constant. The constitutive Eq. (1) thus reduces to

$$\boldsymbol{\sigma} = \tau(\boldsymbol{\sigma})(\mathbb{C}_R + \mathbb{C}_G) : \dot{\boldsymbol{\varepsilon}} \qquad (8)$$

In the case of a positive uniaxial tensile test, $(\boldsymbol{\sigma}_{dev} : \boldsymbol{\sigma}_{dev}) = 2\,\sigma^2/3$ and $p = -\sigma/3$. Then, the glass transition temperature at yielding, as given by Eq. (7), is expressed by the stress component $\sigma = \sigma_Y > 0$ in the loading direction.

$$T_g(\sigma_Y) = T_g^{bulk} - \frac{3+\alpha}{3K}\sigma_Y\ , \qquad (9)$$

with $T_g^{bulk} = T_g^{bulk}(\sigma = 0)$

Combining Eqs. (9) and (3) leads to the following expression:

[1] Pressure–Volume–Temperature

$$\log_{10}\left[\frac{\tau(T,\sigma)}{\tau_g}\right] = -\frac{C_1\left[T-T_g^{bulk}+\frac{3+\alpha}{3K}\sigma_Y\right]}{C_2+\left[T-T_g^{bulk}+\frac{3+\alpha}{3K}\sigma_Y\right]}$$

$$\log_{10}\left[\frac{\tau(T,\sigma)}{\tau_g}\right] \approx -\mathcal{G}_{wlf}\left(T-T_g^{bulk}\right) - \mathcal{G}'_{wlf}\left(T-T_g^{bulk}\right)\frac{3+\alpha}{3K}\sigma_Y \quad (10)$$

The right term of Eq. (10) is obtained by first-order expansion around a given temperature, where

$$\mathcal{G}_{wlf}\left(T-T_g^{bulk}\right) = \frac{C_1\left[T-T_g^{bulk}\right]}{C_2+\left[T-T_g^{bulk}\right]} \text{ and } \mathcal{G}'_{wlf}\left(T-T_g^{bulk}\right) = \frac{d\mathcal{G}_{wlf}}{dT} = \frac{C_1C_2}{\left[C_2+\left(T-T_g^{bulk}\right)\right]^2}$$

Introducing Eq. (10) into Eq. (8) allows us to obtain

$$\sigma_Y e^{A\sigma_Y} = \tau_g\,\dot{\varepsilon}(E_R+E_G)e^{-2.3\,\mathcal{G}_{wlf}\left(T-T_g^{bulk}\right)} \quad (11)$$

with

$$A = 2.3\,\frac{3+\alpha}{3K}\,\mathcal{G}'_{wlf}\left(T-T_g^{bulk}\right) \quad (12)$$

The solution to Eq. (11) can be written using the Lambert or product–log function, which we will denote by W[2]

$$\sigma_Y = \frac{W\left((E_R+E_G)\tau_g\,\dot{\varepsilon}\,A\,e^{-2.3\,\mathcal{G}_{wlf}\left(T-T_g^{bulk}\right)}\right)}{A} \quad (13)$$

For values $10^2 \le x \le 10^9$, the Lambert W is approximated by a natural logarithm, $W(x) \approx a\,ln(x)$, where a varies from 0.74 to 0.86.

[2] The Lambert or product–logarithm function $W(x)$ is defined by the equation $x = W(x)e^{W(x)}$

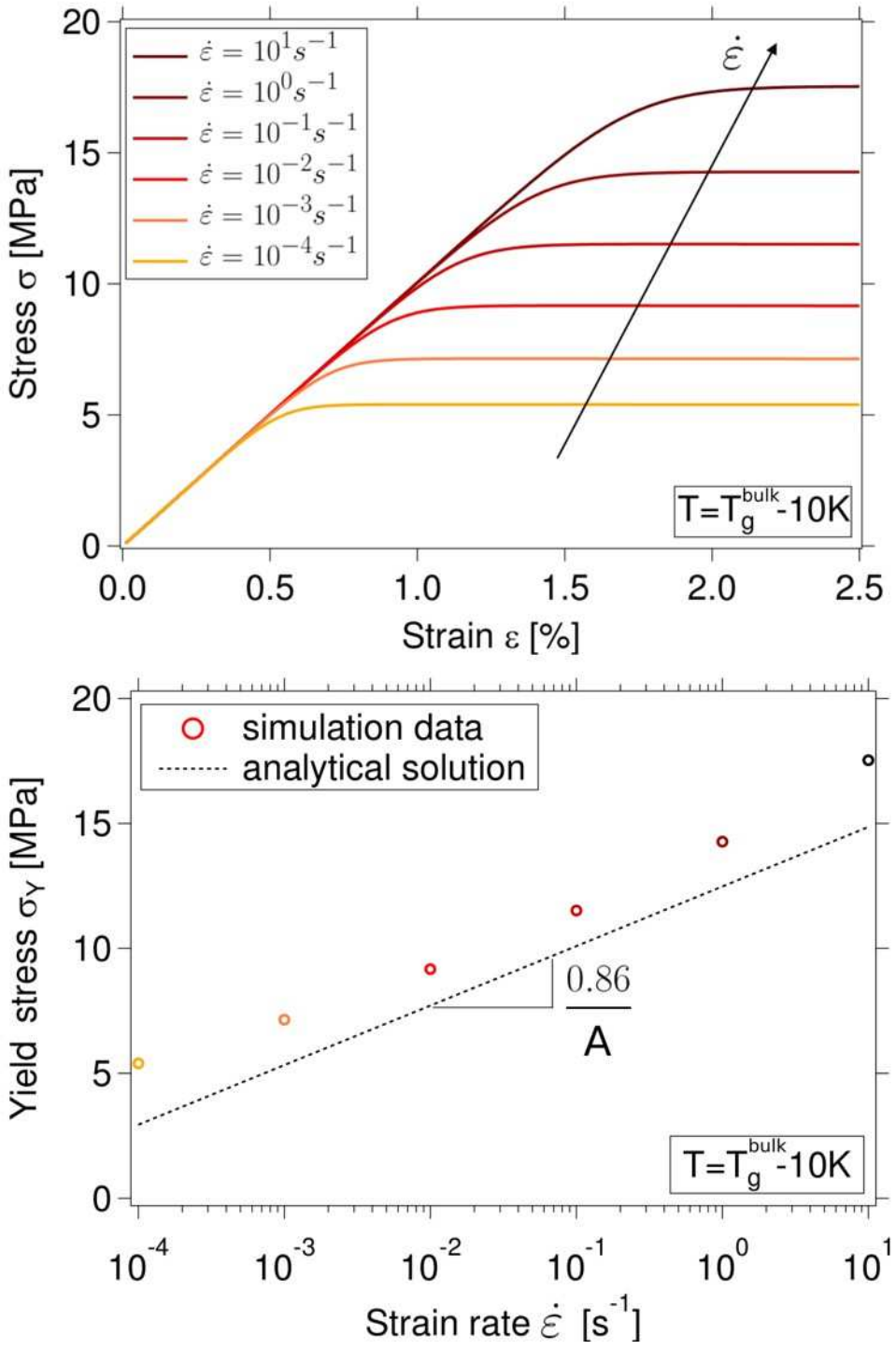

310

Figure 3: Yielding at different strain rates at $T = T_g^{bulk} - 10K$ with $T_g^{bulk} = T_g^{bulk}(\sigma = 0)$: (top) stress–strain graph at various strain rates; (bottom) yield stress as a function of the strain rate in logarithmic scale. Material parameters: E_R =1.0 MPa, E_G =1.0 GPa, T_g^{bulk} = 150 K, C_1 =12.8, C_2 = 34.0 K., K= 1.0 MPa K^{-1}, and α= 0.3.

315

As a consequence, to a good approximation, the yield stress σ_Y is directly proportional to the logarithm of the strain rate $ln(\dot{\varepsilon})$, as shown in Fig. 3:

$$\sigma_Y \approx \frac{0.8}{A} ln(\dot{\varepsilon}) + 0.8 \frac{ln\left((E_R+E_G)\tau_g \; e^{-2.3\, G_{wlf}\left(T-T_g^{bulk}\right)} \right)}{A} \quad (14)$$

The model provides a stress/strain rate response in qualitative agreement with the plastic deformation behavior observed for most glassy polymers at temperatures below T_g^{bulk}. The model also predicts the response measured on real systems in their rubber state and in their glass transition regime. Similarly, it also provides a description of the temperature dependence of the yield stress of glassy polymers. Finally, the complex behavior of a glassy polymer material is simplified here to a unique formulation with a stress-dependent relaxation time.

To complete the description of the polymer chains within confined regions, the stress dependence has been coupled with the filler-matrix interaction effect.

2.3 Coupled local stress and surface confinement law—$T_g(z_i, \boldsymbol{\sigma})$

It will be assumed that the dynamic change resulting from confinement or stress can be written as the addition of the two temperature shifts established above. Hence, we write, from Eq. (5) and Eq. (7):

$$T_g(z_i, \boldsymbol{\sigma}) = T_g(z_1, z_2, \boldsymbol{\sigma}) = T_g^{bulk}\left(1 + \frac{\delta}{z_1} + \frac{\delta}{z_2}\right) - \frac{\sqrt{\frac{3}{2}\boldsymbol{\sigma}_{dev} : \boldsymbol{\sigma}_{dev}} - \alpha\, p}{K} \quad (15)$$

The complex local mechanical behavior of polymer chains confined by filler particles is simplified through a constitutive equation that accounts for both confinement and strain softening effects.

The originality of the proposed approach is to model the shift in the glass transition $T_g(z_i,\ \boldsymbol{\sigma})$ by combining, in a linear manner, the dependence on pressure and strain, which to our knowledge is not common. Moreover, it can be seen that the mechanical behavior has only been described in terms of the polymer matrix properties and filler-matrix interaction. Indeed, the bulk material parameters T_g^{bulk}, α, and K may be measured from the mechanical response of the pure polymer, which is quite unique for a constitutive model for filled elastomers. The last parameter δ is driven by the filler-matrix interaction.

It can only be measured by indirect means, such as NMR or calorimetry (Papon et al., 2012).

As a consequence, the model can be adapted for different matrix-filler interactions and for different aggregate structures, sizes, or concentrations.

3 Cyclic shear response of the model

In this section, the model is applied to simple cyclic loading histories to show the ability of the new model to represent both the effect of temperature in the linear regime and the Payne effect.

For the sake of simplicity, the behavior of the central point is chosen to simulate the confined polymer response, and all numerical simulations have been performed as follows:

—The behavior is represented by an infinitesimal volume at the central middle point of the glassy bridge. Eq. (15) is then reduced to the following:

$$T_g(h(t),\boldsymbol{\sigma}) \approx T_g^{bulk}\left(1+4\frac{\delta}{h(t)}\right)-\frac{\sqrt{\frac{3}{2}\boldsymbol{\sigma}_{dev}:\boldsymbol{\sigma}_{dev}}-\alpha\, p}{K} \quad (16)$$

applying $z_1 = z_2 = h(t)/2$, where $h(t)$ is the glassy bridge height at time t. The initial value of the glassy bridge height is denoted by $h_0 = h(t=0)$

—The bulk material parameters of the model are as follows:

Material parameters		
		Units
E_R	1	MPa
E_G	1000	MPa
C_1	12.8	
C_2	34	K
T_g^{bulk}	150	K
α	0.3	
K	1	MPa K^{-1}
δ	1	nm

—Simulations are performed on a single cubic linear mesh element

—Cyclic shear loadings were performed at zero steady state:

—A sinusoidal displacement in the x-direction $u_x = \Delta\gamma \sin(2\pi f t)$ was applied on the face opposite the *xy*-plane to reproduce simple shear, where *f* is the frequency.

—A vertex of the cube was fixed at the origin, and the three faces lie on the *xy*, *yz*, and *zx*-planes in the undeformed state.

—Displacements in the *y* and *z* directions were blocked on the same face.

—Zero displacements in all directions were imposed on the face lying on the *xy*-plane.

—The same deformation for the cube was imposed to the "fictitious" particles, inducing an increase in $h(t)$. The average strain and stress were computed on the cube.

—Storage (elastic) and loss (viscous) linearized moduli were computed from the first-order terms of the Fourier transform decomposition of the signal after stabilization (3rd cycle). In other words, only the first harmonic of the mechanical response is reported.

3.1 Cyclic stress/strain response of one bridge

To verify the microscopic constitutive law, we performed temperature and shear strain sweep simulations on several single glassy bridges with various heights. We have thus analyzed the effect of confinement and of stress softening on the mechanical response of a polymer bridge.

Fig. 4 shows the local behavior of a bridge for three different scenarios at a given temperature *T,* taken 150 K above the bulk glass transition temperature ($T = T_g^{bulk} + 150$ K), i.e., $T = 300$ K for PDMS chains. The figure presents predictions computed applying a strain amplitude of 0.5%, at which the distance between particles is nearly constant with time $h(t) \approx h_0$.

In the absence of confinement, i.e., $h(t) \approx h_0 \gg \delta$, the glass transition temperature at the center of the bridge is equal to the bulk one T_g^{bulk} according to Eq. (16). The temperature of the experiment T is thus significantly larger than $T_g(h(t), \boldsymbol{\sigma}) = T_g^{bulk}$. According to Eq. 3, the relaxation time does not depend on time and is very short at the

temperature of the experiment T. The polymer response is thus that of the rubber bulk state.

Conversely, confinement results in an increase in the local glass transition defined by $T_g(h(t), \boldsymbol{\sigma} = \mathbf{0})$, which becomes larger than T_g^{bulk}. At temperature T, the dynamics of the polymer chains is thus slowed down compared with that of the bulk polymer, and their relaxation time $\tau(h(t), T, \boldsymbol{\sigma} = \mathbf{0})$, which is predicted by Eq. (3), increases as a result of confinement. Because the distance of the bridge $h(t)$ is nearly constant at the applied strain amplitude, the relaxation time is also constant with time. According to Eq. (5) and assuming a δ value of 1 nm, the glass transition temperature at the center of a 4-nm high bridge is shifted by a factor of two : $T_g(h_0, \boldsymbol{\sigma} = \mathbf{0}) = 2\, T_g^{bulk}$. In this case, Eq. (3) predicts an increase in the relaxation time of 10 decades at a temperature *T* of 300 K (see right inset in Fig. 4).

In the weak deformation regime, stress decreases the T_g shift induced by pure confinement following Eq. (16). In the example presented in Fig. 4, the value of $T_g(h(t), \boldsymbol{\sigma})$ becomes smaller than the temperature of the experiment T.Consequently, the value of the relaxation time becomes close to $1/(2\pi f)$ and the dashpot in our Zener model allows a viscous flow. In addition to the T_g shift induced by confinement, the stress–time dependency term in Eq. (16) modifies the shape of the σ/γ cycle. As a result, the bridge response is both stiffer than in the absence of confinement and viscoelastic.

Finally, the non-linearity of the mechanical response results in the stress dependency of the glass transition. The increase in $\boldsymbol{\sigma}$ with increasing strain amplitude results in a reduction of the relaxation time, which corresponds to a viscoelastic softening, together with a decrease in the elastic modulus and an increase in the viscous modulus (see Fig. 4). As the value of the relaxation time decreases, the value of the tangent modulus—defined as the ratio of the stress amplitude to the strain amplitude—reaches that of the rubbery modulus. Thus, the stress-dependent formulation of the relaxation times defines polymer "pseudo"-plasticity as a time-dependent phenomenon.

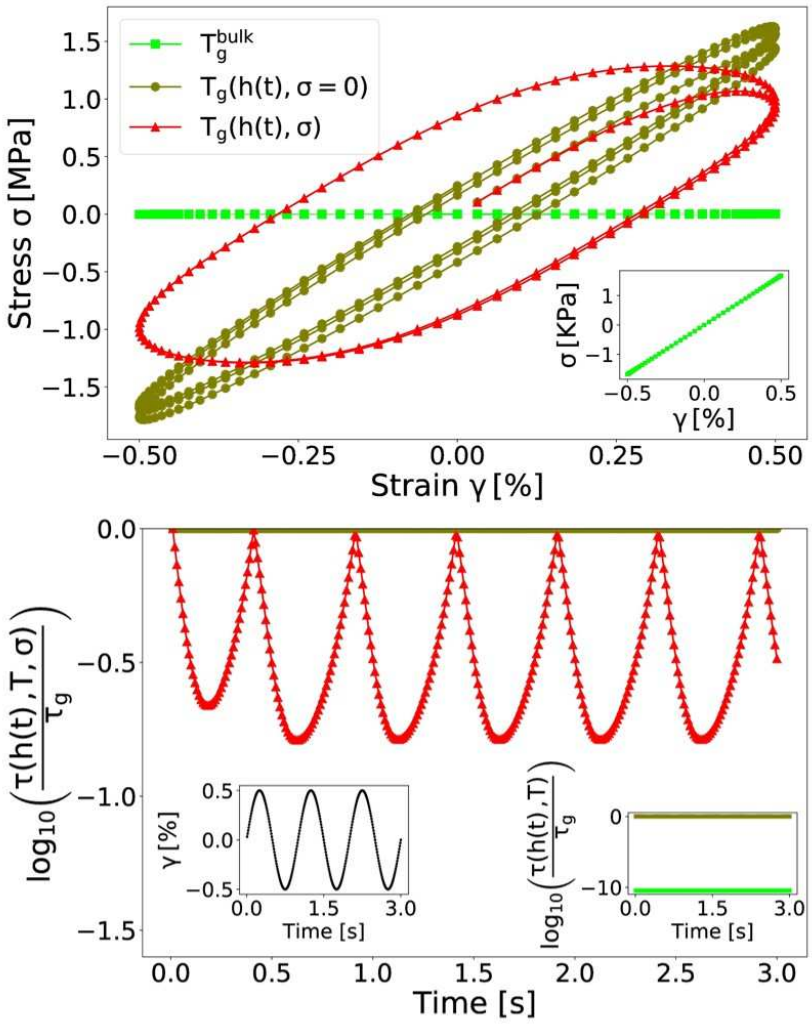

Figure 4: Cyclic stress–strain (top) curve and evolution of relaxation time τ (bottom) with respect to time for the confined polymer behavior at temperature $T = T_g^{bulk} + 150$ K = 300 K and frequency 1 Hz in a cyclic simple shear of 0.5% strain amplitude. Three different cases are plotted. No confinement : $h(t) \to \infty$ .The glass transition at the center of the bridge is equal to T_g^{bulk} and $T \gg T_g^{bulk}$ (green squares). Confinement without stress softening: $h(t) \approx h_0 = 4$ nm and $T = T_g(h(t), \boldsymbol{\sigma} = \mathbf{0})$ (red triangle). Coupling of confinement and stress softening: $h(t) \approx h_0 = 4$ nm and $T \geq T_g(h(t), \boldsymbol{\sigma})$ (brown circle). Material parameters: E_R =1.0 MPa, E_G =1.0 GPa, T_g^{bulk} = 150 K, C_1 =12.8, C_2 = 34.0 K, K= 1.0 MPa K^{-1}, α= 0.3, and δ= 1 nm. The right inset of the figure (bottom) shows the relaxation time of the polymer chains predicted by Eq. (3) assuming no confinement or pure confinement. In the left inset of the figure (bottom), the time history of applied strain is plotted.

3.2 From one bridge to many bridges, effect of cyclic shear

To investigate the collective behavior of a real sample, we determined the average response of an arbitrary uniform distribution of glassy bridge points. Twenty-five separated cubic elements with glassy bridge heights h_0 uniformly distributed between 3 nm and 8 nm were considered. The total response was computed using either a parallel or a series approximation. In the first case, the elements underwent the same sinusoidal deformation cycle, the total stress response being the average of the set of stress outputs. In the second case, the elements underwent the same sinusoidal stress cycle, the total stress response being the average of the set of strain outputs.

3.2.1 Linear regime, effect of temperature

First, in the linear regime, the mechanical response as a function of the temperature for various particle-to-particle distances was computed at a small strain amplitude $\Delta\gamma = 0.01\%$ at frequency $f = 1$ Hz. In that case, the height of a bridge $h(t)$ is nearly constant with time and its value is close to h_0. Moreover, the value of stress felt by the bridge is small. Consequently, the time relaxation does not depend on stress and is constant with time, as shown in right inset of Fig. 4.

Fig. 5 shows the evolution of the relaxation time with respect to the temperature for different $h(t)$, and thus for different $T_g(h(t) \approx h_0)$. For a given bridge height, the glass transition occurs when the value of the relaxation time reaches that of the time-scale defined by the loading $(1/(2\pi f))$. As a result, the transition occurs at higher (lower) temperature as frequency increases (decreases). The model predicts a sharp drop from a glassy storage modulus (~ GPa) to a rubbery one (~ MPa) and a loss modulus maximum that occurs at various temperatures, depending on the distance between particles, as shown in Fig. 5. The shift in the storage modulus drop (and loss modulus maximum) is controlled by the relaxation time, which only depends on the local glass transition temperature. In the linear regime, the local glass transition is driven by the state of confinement h_0. Finally, to show the ability of the model to consider the frequency dependence, cyclic shear loading at two different frequencies, 100 Hz and 0.01 Hz, was applied to a 4-nm high glassy bridge. The frequency dependence is taken into account by the strain rate in Eq. (8). The local relaxation time does not depend on frequency. The responses as a function of the temperature at 100 Hz and 0.01 Hz frequencies (respectively in the dashed line and dotted line) are shown in Fig. 5. Even though they show similar trends, their temperature dependences are different. For instance, the

temperature at which the drop in the storage modulus is observed depends on the frequency.

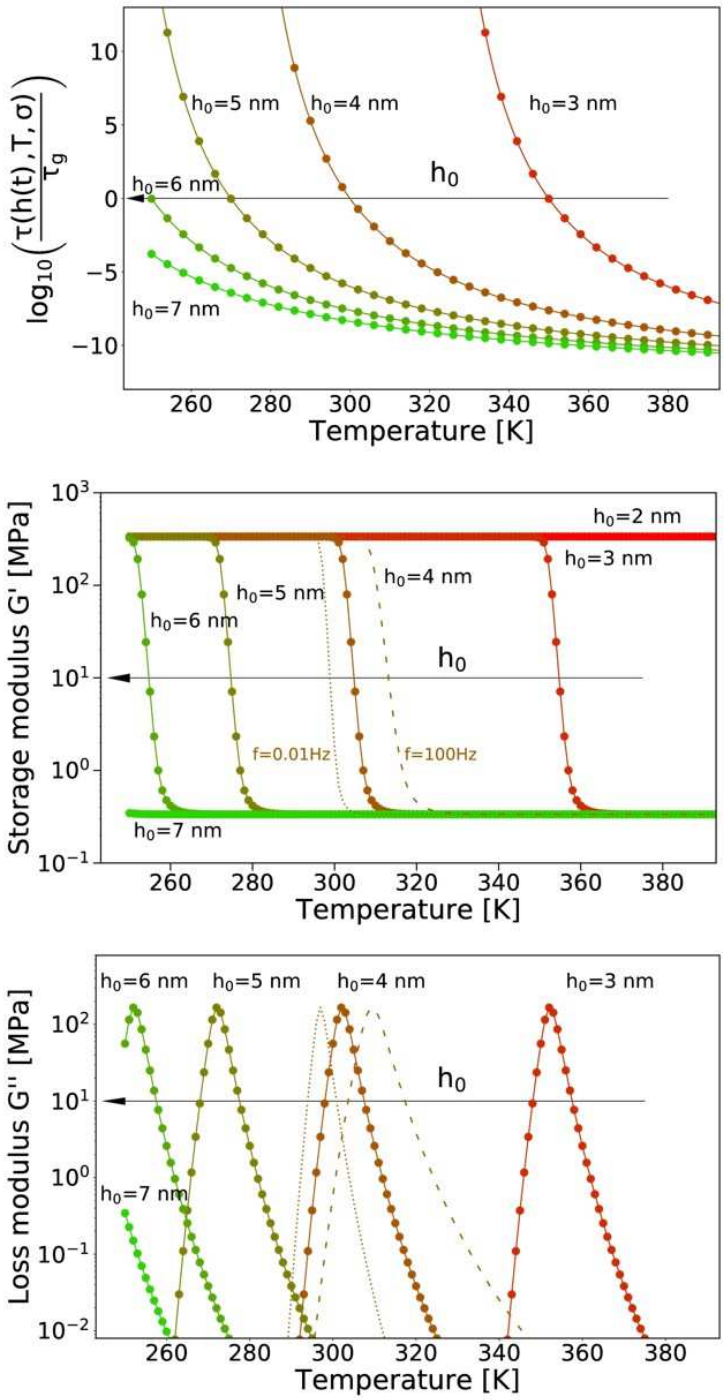

Figure 5: Relaxation time (top), storage modulus (middle), and loss modulus (bottom) as a function of temperature at various glassy bridge heights. Cyclic shear simulations are computed at small strain amplitude $\Delta\gamma = 0.01\%$ and at frequency $f = 1$ Hz. Material parameters: E_R =1.0 MPa, E_G =1.0 GPa, T_g^{bulk} = 150 K, C_1 =12.8, C_2 = 34.0 K, K= 1.0 MPa K^{-1}, α = 0.3, and δ = 1 nm.

Experimentally, at $T < T_g^{bulk} + 50\ K$, a slow decrease in the storage and loss modulus with increasing temperature has been observed with filled systems (Berriot et al., 2002; Fritzsche and Klüppel, 2011), in contrast to the bulk polymer in the absence of fillers. To link the behavior of isolated bridges to real materials, it must be recalled that the macroscopic response of a glassy bridge percolative network is a collective response of a glassy bridge distribution (Montes et al., 2003), i.e., a distribution of h_0. At a given temperature, there is a wide variety of behaviors within the material: from a soft rubbery response to a rigid glassy response going through viscoelastic behavior. By increasing the temperature, a sharp softening of each glassy bridge response occurs for each polymer bridge, as explained above. However, as the height of the bridges is distributed, a slow decrease in the macroscopic modulus of the filled elastomer is observed.

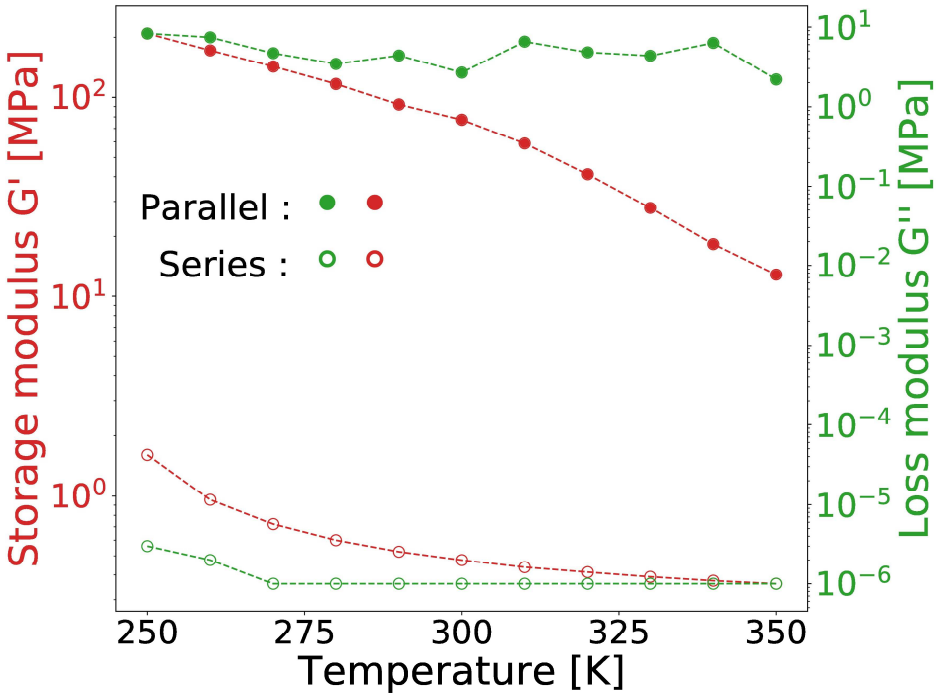

Figure 6: Collective response of a set of glassy bridge, storage modulus (red), and loss modulus (green) as a function of temperature. Cyclic shear simulations are computed at small strain amplitude $\Delta\gamma = 0.01\%$ at frequency $f = 1$ Hz assuming a parallel (solid circles) and series (open circles) approximation. Material parameters: E_R =1.0 MPa, E_G =1.0 GPa, T_g^{bulk} = 150 K, C_1 =12.8, C_2 = 34.0 K, K= 1.0 MPa K^{-1}, α= 0.3, and δ= 1 nm.

Parallel and series approximations are the upper and lower bounds of the expected collective response (see Fig. 6). Here, the order of magnitude of the moduli values did not correspond to experimental data because the description of macroscopic behavior requires a scaling factor that will be discussed in future papers. Nonetheless, the qualitative storage and loss modulus trends are reproduced (Fritzsche and Klüppel, 2011).

3.2.2 Payne effect

Another original feature of a filled elastomer is the strain amplitude non-linearity, called the Payne effect. To test this behavior on a microscopic scale, simulations of the confined cubic element under cyclic simple shear at various amplitudes and at a constant temperature of 300 K were performed.

The evolution of the first-order moduli under shear strain sweep is shown in Fig. 7, for various confinement states. Bridges with large heights have small relaxation times. Consequently, their response is linear and does not depend on stress, as shown for a bridge of 5 nm height in Fig. 7. The value of their storage modulus is equal to that of the rubber modulus, i.e., 0.3 MPa in our work (see the inset of Fig. 7). Bridges at their viscoelastic transition regime in the linear domain ($h_0 = 4$ nm in Fig. 7) are more sensitive to an increase in stress. Their relaxation time is slightly larger or close to the loading frequency in the linear regime. The increase in strain amplitude results in a decrease in the relaxation time. Consequently, the value of the storage modulus decreases and reaches that of the rubber modulus (see the inset of Fig. 7). If their response in the linear domain is close to the elastic glassy behavior, the glassy-to-rubbery transition induced by the strain amplitude goes through a stress–strain cycle opening and a maximum of the loss modulus. As the relaxation time in the linear domain increases, the regime where the bridge response is glassy increases. Thus, the glassy-to-rubbery transition is shifted toward large strain amplitude with a stiffer evolution of properties. This is what is observed for the bridge of 3 nm height in Fig. 7. Finally, linear glassy behavior is observed for strongly confined bridges, for which the glassy feature predominates ($h_0 = 2$ nm in Fig. 7).

At the macroscopic scale, a storage modulus drop and a loss modulus maximum have been observed as a strain amplitude sweep is applied to a filled elastomer (Wang, 1998). The picture we suggest is similar to the one proposed for temperature sweeps: the disorder in the glassy bridges thickness plays a major role. At a given temperature and for small deformations, the global stiffness is determined by a distribution of bridges, mixing

glassy rigid, viscoelastic, and rubbery soft elements. As the strain amplitude increases, the macroscopic response is controlled by the stress softening of a subset of bridges that is in their glassy–rubber viscoelastic transition at the temperature and strain amplitude of the experiment.

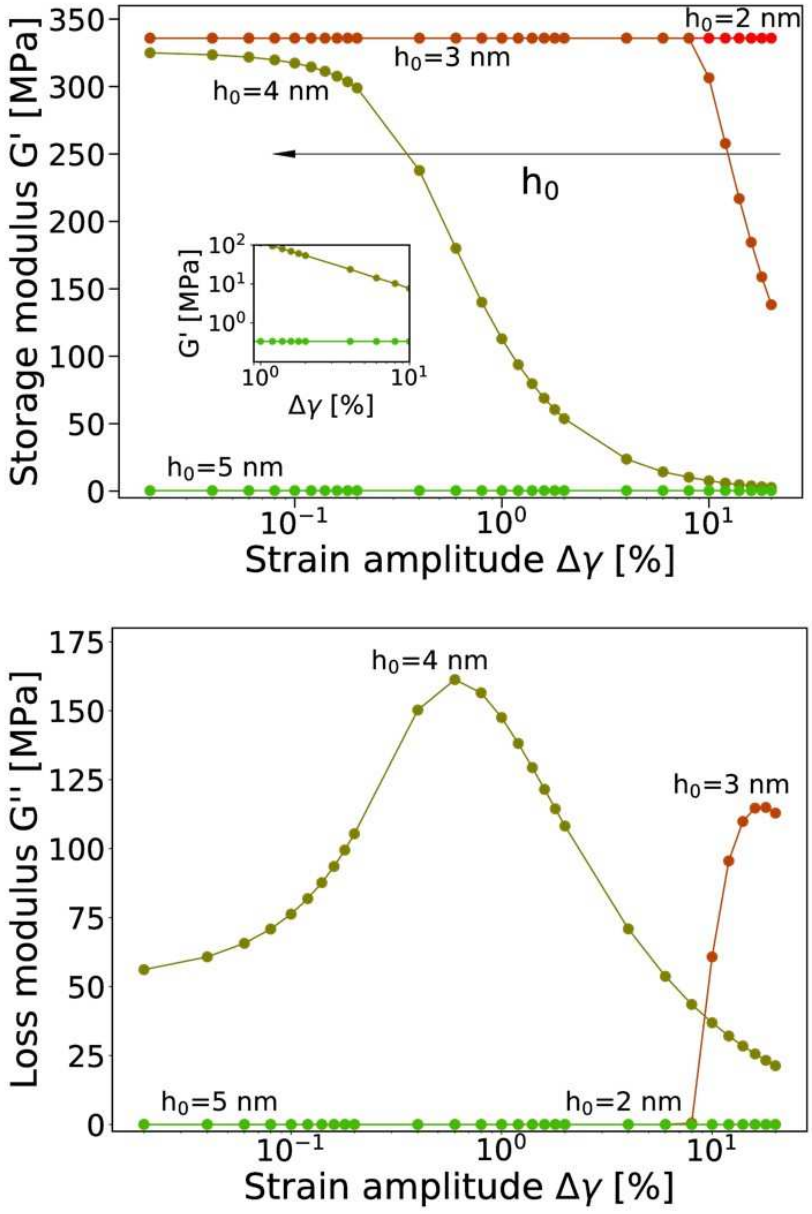

Figure 7: Glassy bridge storage (top) and loss (bottom) moduli as a function of strain amplitude with h_0 values between 3 nm and 8 nm. Cyclic shear simulations are computed at temperature $T = 300$ K and frequency $f = 1$ Hz. Material parameters: E_R =1.0 MPa, E_G =1.0 GPa, T_g^{bulk} = 150 K, C_1 =12.8, C_2 = 34.0 K, K= 1.0 MPa K^{-1}, α = 0.3, and δ = 1 nm.

The response of a collection of glassy bridges under a strain sweep with a distribution of 25 cubic elements, similar to the one used in the temperature-dependent case, is shown in Fig. 8. The resulting response in a parallel approximation exhibits Payne non-linearity. Fig. 9 presents the corresponding stress–strain responses computed at various strain amplitudes compared with the first harmonic contribution of the mechanical response.

At intermediate strain amplitude $\Delta\gamma \leq 2\%$, the stress response is "linear-like" viscoelastic, observed while the storage modulus decreases and the loss modulus increases (see Fig. 8). Indeed, the stress–strain response cycle decreases in slope and increases in hysteresis with a perfectly elliptical shape (see Fig. 9). At larger strain amplitudes close to the characteristic loss modulus maximum, the higher harmonic terms of stress response increase in intensity (see Fig. 9). The behavior becomes doubly non-linear: slope and cycle opening evolve with strain amplitude as well as cycle shape and ellipticity. This peculiar non-linearity is captured by the stress dependence of the relaxation time. Experimentally, these nonlinearities have been observed with filled systems and are referred to as the "harmonic paradox" (Chazeau et al., 2000).

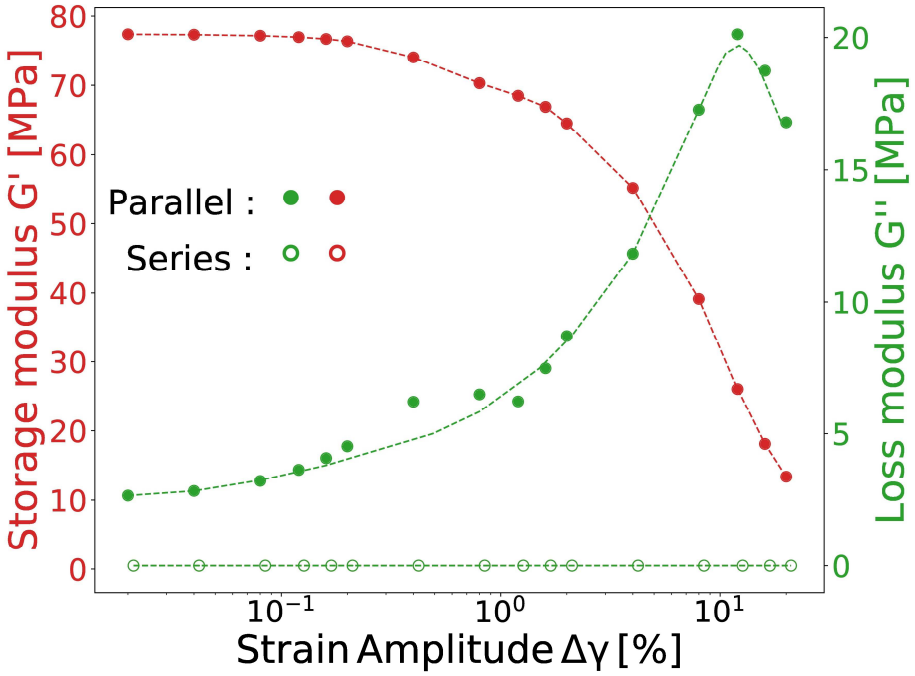

Figure 8: Collective response of a set of glassy bridge, storage moduli (red), and loss modulus (green) as a function of strain amplitude. Cyclic shear simulations are computed assuming parallel (solid circles) and series (open circles) approximation at temperature $T = 300$ K and frequency $f = 1$ Hz. Material parameters: E_R =1.0 MPa, E_G =1.0 GPa, T_g^{bulk} = 150 K, C_1 =12.8, C_2 = 34.0 K, K= 1.0 MPa K^{-1}, α = 0.3, and δ = 1 nm.

However, the series approximation fails to describe the Payne effect. This is due to the contrast in mechanical properties between the elements, which can exceed three decades. We thus foresee considerable difficulties for scaling up the bridge mechanics to the macroscopic scale. The effect of steady loading has not been evaluated in this work. However, the model can be extended to describe situations in which a constant strain is applied in addition to a cyclic strain of large amplitude. In this case, the variables $h(t)$ and $\boldsymbol{\sigma}$ would be modified by the static strain imposed.

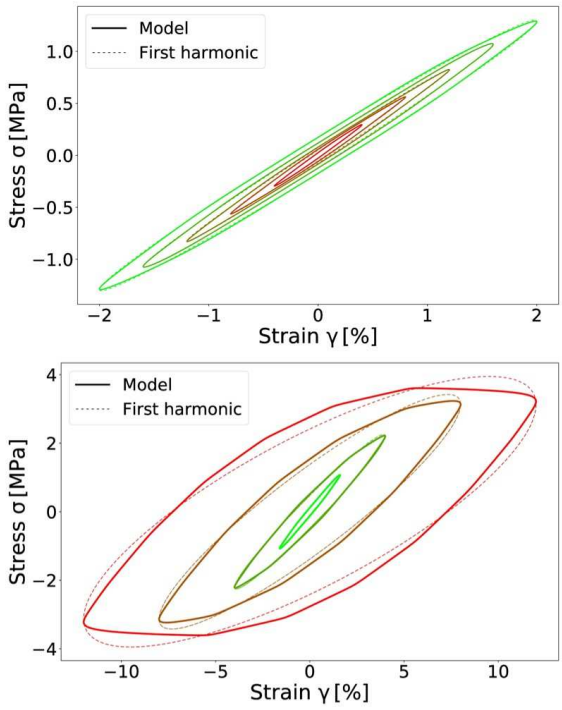

Figure 9: Payne harmonic paradox: Lissajous curves predicted by the model at various strain amplitudes for a set of glassy bridges with heights ranging between 3 nm and 8 nm are plotted with solid lines. The corresponding first-order approximated response (first harmonic) is plotted with dashed lines. At intermediate strains (top) ($\Delta\gamma \leq 2\%$), the stress response is "linear-like" viscoelastic. At higher strains (bottom) ($\Delta\gamma \geq 2\%$), the modulus decrease is accompanied by higher harmonics terms in the stress response. Cyclic shear simulations are computed at temperature $T = 300$ K and frequency $f = 1$ Hz. Material parameters: E_R =1.0 MPa, E_G =1.0 GPa, T_g^{bulk} = 150 K, C_1 = 12.8, C_2 = 34.0 K, K = 1.0 MPa K^{-1}, α = 0.3, and δ = 1 nm.

4 Conclusion

The addition of a filler in an elastomeric matrix has a major effect that extends beyond simple reinforcement, introducing unusual dependencies and non-linearities. This is explained by the influence of the filler-matrix interaction on the dynamic properties of the chains surrounding the inorganic surface. The reduction in mobility results in polymer chains that locally behave as glassy rigid and "pseudo"-plastic material.

In this study, a new constitutive law has been developed to describe the mechanical response of elastomers near filler surfaces, particularly in regions of strong confinement between aggregates. The model presents a two-branch viscoelastic behavior. The first is a simple spring that accounts for rubber elasticity, and the second is a Maxwell element, with a glassy polymer modulus and a characteristic time depending on temperature, distance from the surface, and local stress tensor. The relaxation time is expressed in terms of a local glass transition temperature function.

A single non-linear viscoelasticity parameter replicates the state of confinement and the coupling between temperature dependence and stress softening. A specific application of the law has been studied for the central point of a region connecting two filler particles. On the microscopic scale, the preliminary results, which are based on an understanding of the physics of filled elastomers, qualitatively reproduce the temperature and stress dependencies of the non-linear viscoelasticity. It has been shown, however, that the up-scaling of this model is delicate because of the huge effect of disorder on the mechanical macroscopic behavior. This point will be discussed in detail in a future publication.

References

Andrews, R. D., Kazama, Y., 1967. Rheo-optical properties of polyvinyl chloride films: unplasticized homopolymer. Journal of Applied Physics. 38 (11), 4118-4123.

Batistakis, C., Michels, M. A. J., Lyulin, A. V., 2014. Confinement-induced stiffening of thin elastomer films: Linear and nonlinear mechanics vs local dynamics. Macromolecules. 47 (14), 4690-4703. DOI: 10.1021/ma5003744

Berriot, J., Montes, H., Lequeux, F., Long, D., Sotta, P., 2002. Evidence for the shift of the glass transition near the particles in silica-filled elastomers. Macromolecules. 35 (26), 9756-9762. DOI: 10.1021/ma0212700

Berriot, J., Montes, H., Lequeux, F., Long, D., Sotta, P., 2003. Gradient of glass transition temperature in filled elastomers. Europhysics Letters. 64, 50-56. DOI: 10.1209/epl/i2003-00124-7

Boyce, M. C., Arruda, E. M., 2000. Constitutive models of rubber elasticity: A review. Rubber Chemistry and Technology. 73 (3), 504-523. DOI: 10.5254/1.3547602

Buckley, C. P., Jones, D. C., 1995. Glass-rubber constitutive model for amorphous polymers near the glass transition. Polymer. 36 (17), 3301-3312. DOI: 0.1016/0032-3861(95)99429-X

Cantournet, S., Boyce, M. C., Tsou, A. H., 2007. Micromechanics and macromechanics of carbon nanotube-enhanced elastomers. Journal of the Mechanics and Physics of Solids. 55 (6), 1321-1339. DOI: 10.1016/j.jmps.2006.07.010

Cantournet, S., Desmorat, R., Besson, J., 2009. Mullins effect and cyclic stress softening of filled elastomers by internal sliding and friction thermodynamics model. International Journal of Solids and Structures. 46 (11-12), 2255-2264. DOI: 10.1016/j.ijsolstr.2008.12.025

Cassagnau, P., 2003. Payne effect and shear elasticity of silica-filled polymers in concentrated solutions and in molten state. Polymer. 44 (8), 2455-2462. DOI: 10.1016/S0032-3861(03)00094-6

Chazeau, L., Brown, J. D., Yanyo, L. C., Sternstein, S. S., 2000. Modulus recovery kinetics and other insights into the Payne effect for filled elastomers. Polymer Composites. 21 (2), 202-222. DOI : 10.1002/pc.10178

Cheng, S., Carroll, B., Lu, W., Fan, F., Carrillo, J. M. Y., Martin, H., Holt, A. P., Kang, N. G., Bocharova, V., Mays, J. W., Sumpter, B. G., Dadmun, M., Sokolov, A. P., 2017. Interfacial properties of polymer nanocomposites: Role of chain rigidity and dynamic heterogeneity length scale. Macromolecules. 50 (6), 2397-2406. DOI: 10.1021/acs.macromol.6b02816

Clément, F., Bokobza, L., Monnerie, L., 2005. Investigation of the Payne effect and its temperature dependence on silica-filled polydimethylsiloxane networks. Part I: Experimental results. Rubber Chemistry and Technology. 78 (2), 211-231. DOI: 10.5254/1.3547879

Deng, H., Liu, Y., Gai, D., Dikin, D. A., Putz, K. W., Chen, W., Catherine Brinson, L., Burkhart, C., Poldneff, M., Jiang, B., Papakonstantopoulos, G. J., 2012. Utilizing real and statistically reconstructed microstructures for the viscoelastic modeling of polymer nanocomposites. Composites Science and Technology. 72 (14), 1725-1732. DOI: 10.1016/j.compscitech.2012.03.020

Drozdov, A. D., Dorfmann, A., 2002. The Payne effect for particle-reinforced elastomers. Polymer Engineering & Science. 42 (3), 591-604. DOI: 10.1002/pen.10974

Ferry, J. D., 1980. Viscoelastic Properties of Polymers. John Wiley & Sons.

Forrest, J. A., Dalnoki-Veress, K., Dutcher, J. R., 1997. Interface and chain confinement effects on the glass transition temperature of thin polymer films. Physical Review E. 56 (5), 5705-5716. DOI: 10.1103/PhysRevE.56.5705

Fritzsche, J., Klüppel, M., 2011. Structural dynamics and interfacial properties of filler-reinforced elastomers. Journal of Physics: Condensed Matter. 23 (3), 035104. DOI: 10.1088/0953-8984/23/3/035104

Funt, J. M., 1988. Dynamic testing and reinforcement of rubber. Rubber Chemistry and Technology. 61 (5), 842-865. DOI: 10.5254/1.3536222

Heinrich, G., Kluppel, H., 2004. The role of polymer-filler-interphase in reinforcement of elastomers. KGK Kautschuk Gummi Kunststoffe. 57, 452-454.

Huber, G., Vilgis, T. A., Heinrich, G., 1996. Universal properties in the dynamical deformation of filled rubbers. Journal of Physics: Condensed Matter. 8 (29), L409. DOI : 10.1088/0953-8984/8/29/003

Jean, A., Jeulin, D., Forest, S., Cantournet, S., N'guyen, F., 2011. A multiscale microstructure model of carbon black distribution in rubber. Journal of Microscopy. 241 (3), 243-260. DOI: 10.1111/j.1365-2818.2010.03428.x

Keddie, J. L., Jones, R. A. L., Cory, R. A., 1994. Size-dependent depression of the glass transition temperature in polymer films. Europhysics Letters. 27 (1), 59-64. DOI: 10.1209/0295-5075/27/1/011

Klüppel, M., 2003. The Role of Disorder in Filler Reinforcement of Elastomers on Various Length Scales. In: Capella, B., Geuss, M., Klüppel, M., Munz, M., Schulz, E., Sturm, H. (Eds.), Filler-Reinforced Elastomers/Scanning Force Microscopy. No. 164 in Advances in Polymer Science. Springer Berlin Heidelberg.

Klüppel, M., 2008. Evaluation of viscoelastic master curves of filled elastomers and applications to fracture mechanics. Journal of Physics: Condensed Matter 21 (3), 035104. DOI: 10.1088/0953-8984/21/3/035104

Kraus, G., 1984. Mechanical losses in carbon-black-filled rubbers. Journal of Applied Polymer Science: Applied Polymer Symposium. 39, 75-92.

Lee, H. N., Ediger, M. D., 2010. Interaction between physical aging, deformation, and segmental mobility in poly(methyl methacrylate) glasses. The Journal of Chemical Physics. 133 (1), 014901. DOI: 10.1063/1.3450318

Lion, A., Kardelky, C., 2004. The Payne effect in finite viscoelasticity: constitutive modelling based on fractional derivatives and intrinsic time scales. International Journal of Plasticity. 20 (7), 1313-1345. DOI: 10.1016/j.ijplas.2003.07.001

Long, D., Lequeux, F., 2001. Heterogeneous dynamics at the glass transition in van der Waals liquids, in the bulk and in thin films. The European Physical Journal E. 4 (3), 371-387. DOI: 10.1007/s101890170120

Loo, L. S., Cohen, R. E., Gleason, K. K., 2000. Chain mobility in the amorphous region of nylon 6 observed under active uniaxial deformation. Science. 288 (5463), 116-119. DOI: 10.1126/science.288.5463.116

Maier, P., Goritz, D., 1996. Molecular interpretation of the Payne effect. Kautschuk Gummi Kunststoffe. 49 (1), 18-21.

Marcadon, V., Herve, E., Zaoui, A., 2007. Micromechanical modeling of packing and size effects in particulate composites. International Journal of Solids and Structures. 44 (25-26), 8213-8228. DOI: 10.1016/j.ijsolstr.2007.06.008

Mark, J. E., Erman, B., Roland, M., 2013. The Science and Technology of Rubber. Academic Press.

Martinez, J. M., Boukamel, A., Méo, S., Lejeunes, S., 2011. Statistical approach for a hyper-visco-plastic model for filled rubber: Experimental characterization and numerical modeling. European Journal of Mechanics - A/Solids. 30 (6), 1028-1039. DOI: 10.1016/j.euromechsol.2011.06.013

Masurel, R. J., Cantournet, S., Dequidt, A., Long, D. R., Montes, H., Lequeux, F., 2015. Role of dynamical heterogeneities on the viscoelastic spectrum of polymers: A stochastic continuum mechanics model. Macromolecules. 48 (18), 6690-6702. DOI: 10.1021/acs.macromol.5b01138

Medalia, A. I., 1986. Electrical conduction in carbon black composites. Rubber Chemistry and Technology. 59 (3), 432-454.

Merabia, S., Sotta, P., Long, D. R., 2008. A microscopic model for the reinforcement and the nonlinear behavior of filled elastomers and thermoplastic elastomers (Payne and Mullins Effects). Macromolecules. 41 (21), 8252-8266. DOI: 10.1021/ma8014728

Montes, H., Chaussée, T., Papon, A., Lequeux, F., Guy, L., 2010. Particles in model filled rubber: Dispersion and mechanical properties. The European Physical Journal E. 31 (3), 263-268. DOI: 10.1140/epje/i2010-10570-x

Montes, H., Lequeux, F., Berriot, J., 2003. Influence of the glass transition temperature gradient on the nonlinear viscoelastic behavior in reinforced elastomers. Macromolecules. 36 (21), 8107-8118. DOI: 10.1021/ma0344590

Mujtaba, A., Keller, M., Ilisch, S., Radusch, H. J., Beiner, M., Thurn-Albrecht, T., Saalwächter, K., 2014. Detection of surface-immobilized components and their role in viscoelastic reinforcement of rubber silica nanocomposites. ACS Macro Letters. 3 (5), 481-485. DOI: 10.1021/mz500192r

Nguyen, H. K., Liang, X., Ito, M., Nakajima, K., 2018. Direct mapping of nanoscale viscoelastic dynamics at nanofiller/polymer interfaces. Macromolecules. 51 (15), 6085-6091. DOI: 10.1021/acs.macromol.8b01185

Nguyen, H. K., Sugimoto, S., Konomi, A., Inutsuka, M., Kawaguchi, D., Tanaka, K., 2019. Dynamics gradient of polymer chains near a solid interface. ACS Macro Letters. 8 (8), 1006-1011. DOI: 10.1021/acsmacrolett.9b00351

Omnès, B., Thuillier, S., Pilvin, P., Grohens, Y., Gillet, S., 2008. Effective properties of carbon black filled natural rubber: Experiments and modeling. Composites Part A: Applied Science and Manufacturing. 39 (7), 1141-1149. DOI: 10.1016/j.compositesa.2008.04.003

Papakonstantopoulos, G. J., Doxastakis, M., Nealey, P. F., Barrat, J. L., de Pablo, J. J., 2007. Calculation of local mechanical properties of filled polymers. Phys. Rev. E. 75, 031803. DOI: 10.1103/PhysRevE.75.031803

Papon, A., Merabia, S., Guy, L., Lequeux, F., Montes, H., Sotta, P., Long, D. R., 2012. Unique nonlinear behavior of nano-filled elastomers: From the onset of strain softening to large amplitude shear deformations. Macromolecules. 45 (6), 2891-2904. DOI: 10.1021/ma202278e

Payne, A. R., 1962. The dynamic properties of carbon black-loaded natural rubber vulcanizates. Part I. Journal of Applied Polymer Science. 6 (19), 57-63.

Ramier, J., Gauthier, C., Chazeau, L., Stelandre, L., Guy, L., 2007. Payne effect in silica-filled styrene\butadiene rubber: Influence of surface treatment. Journal of Polymer Science Part B: Polymer Physics. 45 (3), 286-298. DOI: 10.1002/polb.21033

Ree, T., Eyring, H., 1955. Theory of non-Newtonian flow. I. Solid plastic system. Journal of Applied Physics. 26 (7), 793-800.

Robertson, R. E., 1966. Theory for the plasticity of glassy polymers. The Journal of Chemical Physics. 44 (10), 3950-3956.

Rottler, J., Robbins, M. O., 2001. Yield conditions for deformation of amorphous polymer glasses. Physical Review E. 64 (5), 051801. DOI: 10.1103/PhysRevE.64.051801

Schapery, R. A., 1969. On the characterization of nonlinear viscoelastic materials. Polymer Engineering & Science. 9 (4), 295-310.

Simo, J. C., Hughes, T. J. R., 2006. Computational Inelasticity. Springer Science & Business Media.

Sodhani, D., Reese, S., 2014. Finite element-based micromechanical modeling of microstructure morphology in filler-reinforced elastomer. Macromolecules. 47 (9), 3161-3169. DOI: 10.1021/ma402404x

Treloar, L. R. G., 2005. The Physics of Rubber Elasticity. OUP Oxford.

Van Zanten, J. H., Wallace, W. E., Wu, W.-l., 1996. Effect of strongly favorable substrate interactions on the thermal properties of ultrathin polymer films. Physical Review E. 53 (3), R2053-R2056. DOI: 10.1103/PhysRevE.53.R2053

Vogt, B. D., 2018. Mechanical and viscoelastic properties of confined amorphous polymers. Journal of Polymer Science Part B: Polymer Physics. 56 (1), 9-30. DOI: 10.1002/polb.24529

Wallace, W. E., van Zanten, J. H., Wu, W. L., 1995. Influence of an impenetrable interface on a polymer glass-transition temperature. Physical Review E. 52 (4), R3329-R3332. DOI: 10.1103/PhysRevE.52.R3329

Wang, M. J., 1998. Effect of polymer-filler and filler-filler interactions on dynamic properties of filled vulcanizates. Rubber Chemistry and Technology. 71 (3), 520-589. DOI: 10.5254/1.3538492

Wood, C. D., Chen, L., Burkhart, C., Putz, K. W., Torkelson, J. M., Brinson, L. C., 2015. Measuring interphase stiffening effects in styrene-based polymeric thin films. Polymer. 75, 161-167. DOI: 10.1016/j.polymer.2015.08.033

Zhou, Z., Chudnovsky, A., Bosnyak, C. P., Sehanobish, K., 1995. Cold-drawing (necking) behavior of polycarbonate as a double glass transition. Polymer Engineering & Science. 35 (4), 304-309. DOI: 10.1002/pen.760350404